Available online at www.sciencedirect.com

ScienceDirect

Materials Today: Proceedings 3 (2016) 2713–2724

materialstoday: PROCEEDINGS

www.elsevier.com/locate/procedia

6th International conference on Advanced Nano Materials Title

The Influence of Al_2O_3 Content on ZrO_2-Al_2O_3 Nanocomposite Formation - The Comparison between Sol-Gel and Microwave Hydrothermal Methods

Iwona E. Malka[a,*], Anna Danelska[a], Giora Kimmel[b]

[a]*Institute of High Pressure Physics, Polish Academy of Sciences, Sokolowska 29/37, 01-142 Warsaw, Poland*
[b]*Ben-Gurion University of the Negev, Beer Sheva, 8410501, Israel*

Abstract

Compositions of ZrO_2-Al_2O_3 nanocomposites in the range 10 to 90% wt. of Al were obtained using microwave hydrothermal (MW) synthesis, and sol-gel (SG) method. The use of nanomaterial components as starting ingredients yielded a new nanocomposite material were t-ZrO_2 is stabilized by Al_2O_3 presence after annealing up to 1450°C. Characterization of nanopowders was conducted using X-Ray diffraction (XRD), differential scanning calorimetry and termogravimetry (DSC-TG) methods, specific surface area measurement by BET, density, Raman spectroscopy, and by scanning electron microscopy (SEM). The MW synthesis produces more consistent samples then SG method which yield in amorphous product. All powders after heating up to 1450^{o}C showed fully crystalline phases where the amount of t-ZrO_2 increased with increasing percentage quantity of Al (isolation effect).

Selection and Peer-review under responsibility of the Conference Committee of 6th International Conference on Advanced Nano Materials.

Keywords: Microwave hydrotermal synthesis; sol-gel method; ZrO_2-Al_2O_3 nanocomposites; nanomaterials; phase composition; thermal stability;

* Corresponding author. Tel.: +48-22-888-00-74; fax: +48-22-632-42-18.
E-mail address: iwona@unipress.waw.pl

Selection and Peer-review under responsibility of the Conference Committee of 6th International Conference on Advanced Nano Materials.

1. Introduction

Nomenclature

d_{BET}	average particle diameter calculated using SSA_{BET} value
SSA_{BET}	specific surface area calculated using BET isotherm
ρ	material density

Recently, nanomaterials have sparked a worldwide interest due to their unique physical and chemical properties in comparison to the bulk counterparts. Each innovation lead to the necessity of a fundamental understanding of the phenomena, and the mechanisms associated with them. The need to investigate different alumina-based nanomaterials was raised recently in COST (European Cooperation in the field of Scientific and Technical Research) memorandum [1]. Depending on the size, the material properties and structure can be tailored for specific industrial applications.

Another important material for engineering use is zirconia. Due to its high hardness, high fracture toughness. high melting point, and biocompatibility it is found in application from bio-implants to functional ceramics. It has three polymorphic phases: monoclinic, stable up to 1170°C, tetragonal, stable up to 2370°C and cubic, stable up to 2715°C [2]. Usually, the tetragonal phase is obtained by doping zirconia with rare earth ions at the high temperatures. Stabilized zirconia can be processed in a wide temperature range without phase transformations, which is especially important for sintering. The specific volume of m-ZrO_2 is ca. 2.5% higher than the volume of t-ZrO_2; therefore cracks come into view during sintering of unstabilized zirconia.

The most common stabilizer is Y_2O_3 CaO, MgO and rare earth oxides [2-3]. However, for grain sizes less than 30 nm, the tetragonal phase is stable at room temperature without any stabiliser. This is because the surface energy of the tetragonal phase is lower than for the monoclinic one, and for nano-sized materials it is a large fraction of energy. In practice, however, m-ZrO_2 phase is often obtained using undoped zirconia powders after calcination because of higher crystallite growth rate compared with doped zirconia [4].

Aluminium as a stabilizer of the tetragonal phase is less expensive than the conventionally used Ytria and other rare earth ions. Recent studies suggest that mechanical properties of Al_2O_3– ZrO_2 composites could be considerably improved by reducing the grain size and increasing mixing. Al_2O_3–ZrO_2 composites can be obtained if an amount of tetragonal phase with the ability to transform under applied stress is retained at room temperature [5-6]. To meet this requirement, the size of zirconia grain must be smaller than a critical size (30 nm) to ensure the stability of tetragonal phase at room temperature [7-9].

Zirconia-alumina (ZrO_2-Al_2O_3) nanocomposites are considered amongst other advanced ceramics due to their superior mechanical properties and chemical inertness. They are used for a wide range of applications such as bio-medical implants [10-11] and structural ceramics [12-13].

The grain size was found to be the factor controlling the transition between the zirconia-like and alumina-like phases [14-17]. In our previous work [18] found that the quasi-amorphous phase is formed first, due to its smaller surface energy. It is suggested to use the grain size as a thermodynamic factor, whereby phases conventionally regarded as metastable are considered as stable phases confined to a range of grain sizes. However, obtaining ZrO_2-Al_2O_3 system with full control of particle size of both phases and stabilization of t-ZrO_2 remains a challenge.

To provide optimal performance, the scale reduction of the initial powder or of the final grain morphology is of particular importance [1]. For this reason controlling the structure and properties of the ZrO_2-$A_{l2}O_3$ nanoparticles would be a breakthrough.

Using sol-gel method ZrO_2-Al_2O_3 nanopowders were obtained in wide molar range of composition [18]. We found that in low annealing temperature quazi-amorphous powder is formed. Above 25% Al traces of t-ZrO_2 are visible, and below 25% of Al ZrO_2-Al_2O_3 solid solution exists [18]. It was noted, that increasing of particle size lead to a transition from t-ZrO_2 to m-ZrO_2 which was observed for ZrO_2-1%Al_2O_3 composition after annealing at 900°C. We find that it is possible to stabilize t-ZrO_2 phase in some cases by addition of Al_2O_3. Al_2O_3 presence should prevent t-ZrO_2 particles before growing and at the same time it stabilizes this phase. This is possible even in 1300-1500°C temperature range because the isolation of t-ZrO_2 particles has place [18].

Our strategy regarding the ZrO_2-Al_2O_3 system is to confirm previous findings for various ZrO_2-Al_2O_3 compositions using materials synthesised by two popular methods: sol-gel and microwave hydrothermal synthesis. We will discuss characterization results for ZrO_2-Al_2O_3 powders in a wide range of compositions (form 10 to 90% of Al).

2. Experimental

2.1. Materials

Various compositions of ZrO_2-Al_2O_3 nanopowders were synthesized using microwave- hydrothermal reaction and sol-gel method. The reagents used in the process were the following: Zirconyl chloride octahydrate ($ZrOCl_2 \cdot 8H_2O$ Sigma-Aldrich (≥99.5%)), Sodium hydroxide (CHEMPUR, analytically pure), and Aluminium nitrate nonahydrate ($Al(NO_3)_3 \cdot 9H_2O$ CHEMPUR, analytically pure). The materials were used to prepare 120 ml of 0.5 M $ZrOCl_2 \cdot 8H_2O$ (0.06 moles of $ZrOCl_2 \cdot 8H_2O$), and 400 ml of 2.0 M NaOH. $Al(NO_3)_3 \cdot 9H_2O$ which was dissolved directly in 0.5 M $ZrOCl_2 \cdot 8H_2O$ solution.

Sodium hydroxide solution was added dropwise under a pH-meter control at 25.0ºC. The suspension was stirred by using of a magnetic stirrer (200-500 RPM depending on suspension viscosity and volume). Batches of different ZrO_2-Al_2O_3 compositions were prepared. Every batch with a set composition ZrO_2-Al_2O_3 was divided in two parts in order to obtain two groups with 6 samples in each one. The details of composition are presented in table 1. Different co-precipitation processes were applied for the solutions of these groups, resulting in two kinds of products. Group 1, represents microwave hydrothermal synthesis applied directly to the solution. Group 2 are powders prepared by sol-gel technique. In the second method the solid particles were separated from the liquid by filtration. The gel was then dried at 60 ℃ for 24-48 h yielding the initial sol-gel product (xerogel).

Table 1. Synthesized ZrO_2-Al_2O_3 compositions.
Where: m% Al is wt.% of Al in ZrO_2-Al_2O_3 system.

Sample No.	m % Al	Sample name
1	0.0	ZrO_2
2	9.6	10%Al
3	29.9	30% Al
4	62.5	60% Al
5	80.0	80% Al
6	90.9	90% Al

Microwave reaction took part in a MAGNUM II ERTEC microwave reactor (2.45 GHz, 600 W). The reaction parameters were set as follows: T = 258-263°C, P = 50-56 atm, heating time = 20 min. The product of microwave-assisted hydrothermal reaction was washed on a filter paper with deionized water and isopropanol. Then, powders were left to dry on the filters at room temperature. The collected material was washed in ethanol and again left to dry at room temperature for 24 h.

2.2 Methods

SEM analysis of ZrO_2-Al_2O_3 powders was performed on carbon-coated samples using Ultra Plus scanning electron microscope from Zeiss.

TG-DSC analysis was carried out by using of a STA 449 F1 Jupiter by Netzsch. The analysis was performed with a heating rate of 10°C/min; the top temperature was 1450°C. The measurement was performed in the constant flow of helium: 60 ml/min.

X-ray diffraction patterns of nanopowders were collected on X'Pert PRO, PANalytical diffractometer equipped with a copper anode ($CuK\alpha_1$) and an ultra-fast PIXcel^{1D} detector. The analysis was performed at room temperature in the 2θ range 10°–90° with a step of 0.03°.

Density measurements of samples were carried out by using of a helium pycnometer (AccuPyc 1330, Micromeritics) by adapting an in-house measurements procedure.

Specific surface area of the nanopowders was measured by the BET isotherm method using Gemini 2360 instrument by Micromeritics. Before the density and SSA_{BET} measurements were taken, the powders had been dried at 220°C for 2 h in a constant flow of helium. The average diameter of the particles (d_{BET}) was computed on the basis of SSA_{BET} and density (1) assuming that all of the ZrO_2 particles are spherical and identical.

$$d_{BET}[nm] = \frac{6000}{SSA_{BET}\left[\frac{m^2}{g}\right] \cdot \rho\left[\frac{g}{cm^3}\right]} \quad (1)$$

where:
d_{BET} – average particle diameter calculated using SSA_{BET} value [nm];
SSA_{BET} – specific surface area calculated using BET isotherm [m^2/g];
ρ – material density [g/cm^3];

Chemical composition of samples was investigated using Raman scattering spectroscope (Horiba-Jobin-Yvon LabRam HR a confocal microscope) equipped with a Quantum 95 Ventus 532 nm laser at 150 mW. Experiments were performed at room temperature with a back scattering geometry. The acquisition time was 4 s. Raman analyses were performed with a spectral resolution of 1 cm^{-1}. The spectra were recorded in the range of 50–4000 cm^{-1} using 514.5 nm excitation wavelengths source.

3. Results and Discussion

3.1. Characteristic of as-synthesized nanopowders

The results presented in table 2 show that SG nanopowders have lower density than MW nanocomposites. The difference in apparent density may be explained by the presence of surface impurities in SG samples while MW sample particle surfaces are clean. As a result a closer packing of particles is expected in MW case. In addition, the particles size and BET specific surface area for SG nanopowders is not monotonic and varies a lot with %Al while particle size and SSA from BET on MW samples shows clear trend.

Table 2. SSA_{BET}, d, and particle size of ZrO_2-Al_2O_3 samples obtained MW and SG methods.

	SOL-GEL SAMPLES			MICROWAVE SAMPLES		
	Density (g/cm^3)	BET surface area (m^2/g)	Particle size (BET) (nm)	Density (g/cm^3)	BET surface area (m^2/g)	Particle size (BET) (nm)
ZrO_2	4.65	204	6.3	5.17	114	10.1
10%Al	4.26	175	8.0	5.08	138	8.6
30%Al	3.66	62	28.3	4.58	146	9.0
60%Al	3.42	282	6.2	3.94	124	12.3
80%Al	2.95	110	18.5	3.49	119	14.5
90%Al	2.88	197	10.6	3.23	78	23.7

Analysis of results given in table 2 leads to a simple conclusion: the more consistent and homogeneous results for nanopowders are obtained by MW synthesis. This method brings production of nanoparticles in the particle size range from 9 to 24 nm. Specific surface area was in range from 78 to 146 m^2/g. These comparisons confirm that microwave hydrothermal method creates more uniform, reproducible nanoparticles [19].

Figure 1 shows SEM images for as-prepared nanopowders using MW and SG methods. For the lower amounts of Al (10-30%) in the composite there is no visible influence of synthesis way on powders morphology.

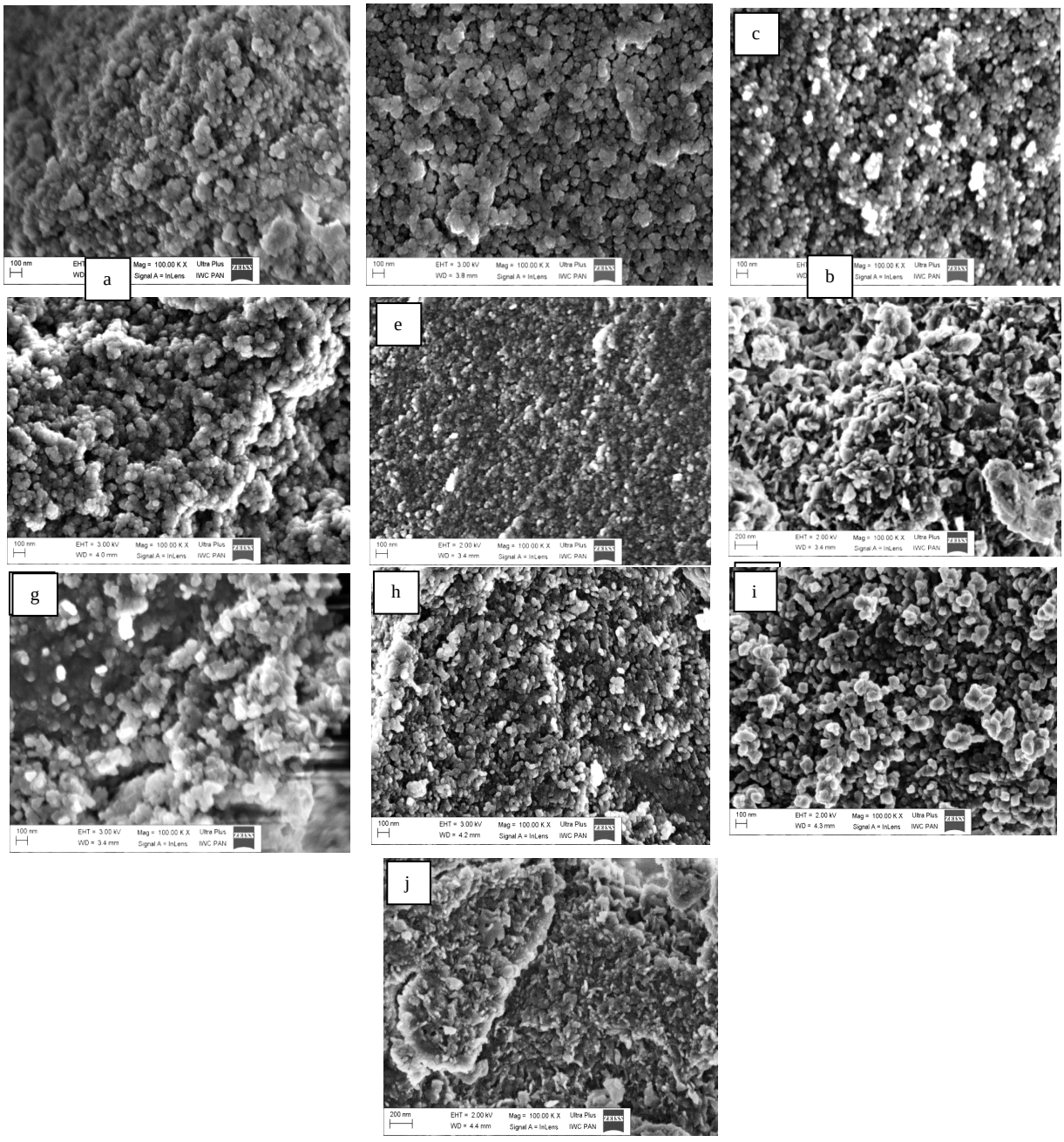

Figure 1. SEM images for nanopowders obtained by MW method, where (a) is 10% Al, (c) 30%Al, (e) 60%Al, (g) 80%Al, (i) 90%Al. SEM images of nanopowders produced by SG method: (b) 10%Al, (d) 30%Al, (f) 60%Al, (h) 80%Al, and (j) 90%Al.

The SEM images for SG samples with 60% (f) and 90% (j) of Al have “flake-like” features. This coincides with high SSA BET measurements in Table 2.

Figure 2 shows XRD patterns for as-synthesied SG and MW nanocomposites. In case of MW powders all products were crystalline phases. The diffractograms with distinct diffraction lines are shown in Fig. 2-a. In the pure zirconia (sample 1) the major phase is the tetragonal zirconia with some monoclinic zirconia. In the sample 2 there is also lack of Al phase, and the amount of the monoclinic phase drops. From samples 2 up to 6 (30-90% of Al) AlOOH precipitate in boehmite structure is visible. The width of the diffraction line indicate that the zirconia

crystals are in the nano range (grain size ~ 10-30 nm). However, the boehmite showed larger grain size (above 100 nm). Rietveld analysis (not shown here) yields increasing amount of AlOOH and decreasing of the relative amount of the monoclinic phase in the ZrO_2 compound versus the amount of Al in the prepared samples. The unit cell parameters of the Zr-Al-O phases were different from those with pure zirconia. The amount of the boehmite increases with the amount of Al in the samples as shown in Fig. 2-c.

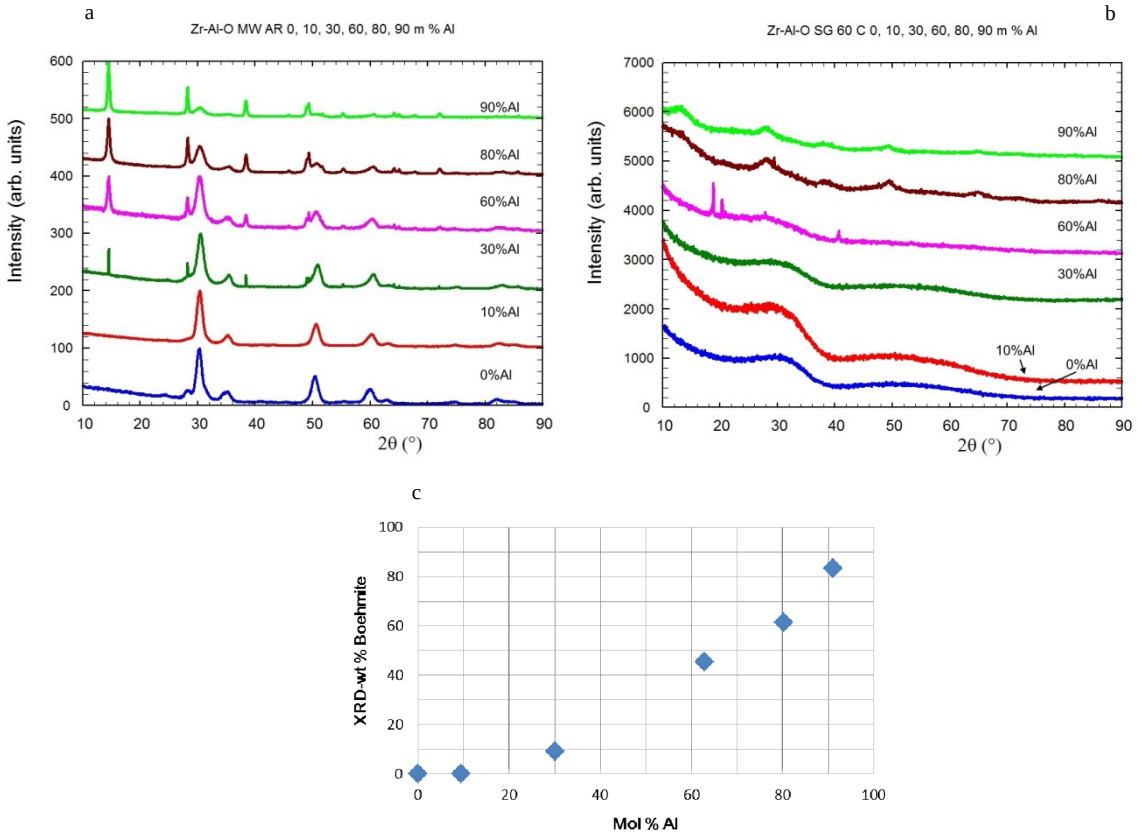

Figure 2. XRD patterns for as-synthesied ZrO_2-Al_2O_3 MW (a), and SG powders. Pure Zr is in the bottom and 90 mol % Al is in the top. Fig. 2-c represents amount of Boehmite in ZrO_2-Al_2O_3 powders synthesied by MW method.

Pure zirconia and the prepared compositions of 10 and 30 % Al by SG method do not show any Bragg peaks (Fig.2-a). These spectra are typical to quasi amorphous zirconia. The diffractogram of sample no 4 (prepared as 60 % Al) shows some sharp diffraction lines belong to $Al(OH)_3$ – bayerite. The diffractograms of samples no. 5 and 6 (prepared as 80 and 90 of %Al, respectively) show boehmite. Its diffraction peaks were severely broadened, indicating precipitation of nanocrystalline AlOOH.

Figure 3 represents Raman spectra. All powders show C-O-C asymmetric vibration in the range 1060-1150cm^{-1}, and weak V(O-H) bands in the range: 3100-3650cm^{-1}. Bands visible on Fig.3-a in the range 2800-3000cm^{-1} may originate from isopropanol used for washing freshly made powders directly after synthesis. Below 1000cm^{-1} in both cases M-O bands are present. However, they can be clearer distinguished in case nanopowders obtained by MW method. According to results reported by Stefanic et al. the Raman spectroscopy of pure metastable tetragonal zirconia exhibits all or some of the following bands: 642, 463, 314, 267 and 147 cm^{-1} [20]. The existence of any dopants results in a shift in the mentioned bands. On the other hand, Yashima et al. [21] show that the intensity ratio of pure and stabilized phases is different. They observed that the intensity ratio of the band at approximately 460 and 640 cm^{-1} increases from zero at 20 mol% dopant (cubic phase) to approximately 0.35 at 6 mol%.

This change is attributed by the authors to be a function of oxygen displacement along the *c*-axis in the unit cell, which increases with decreasing dopant. In both cases ZrO_2 spectra's are consistent with the 10%Al. Changes in Raman patterns become visible only from 30% Al content.

Fig. 3-b shows that additive of 30% of Al shifts bands to the right relative to ZrO_2 and 10% Al. For 60% Al bands at 380 and 500cm^{-1} appear and for 80-90%Al additional bands at: 420, and 690cm^{-1} are visible. Raman vibrations of Al-O bonds are present at approximately 380, 410, 605, and 630cm^{-1} [22-24].

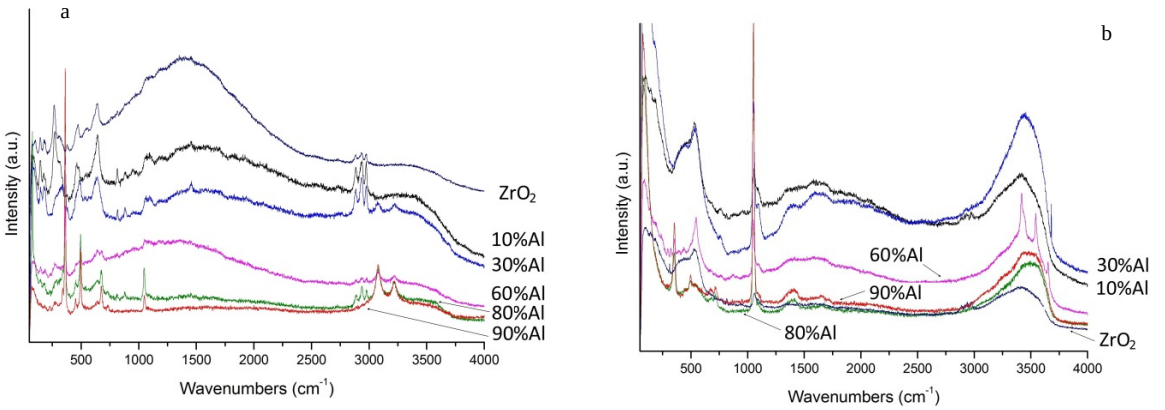

Figure 3. Raman spectra for as received ZrO_2-Al_2O_3 nanopowders obtained by (a) MW, and (b) SG method.

The thermal behaviour of nanocomposites received using MW and SG method is shown in Fig.4. DSC signals for sol-gel powders are characterized by 2 events: 500-750^oC and 1100-1300^oC (Fig.4-b). The sample with 10% of Al shows additional endothermic transition in the range: 250-400^oC. This transition is the most likely connected to evaporation of water. The signal in the range: 500-750^oC is due to the CO_2 desorption which was confirmed by STA-MS investigation (we examined 10%Al, as a representative sample. However, results are not shown here). This transition has its reflection in TG signals (Fig.4-d). The second endothermic event around approximately 1100^oC is due to particle growth and further (t→m) ZrO_2 phase transformation. The MW nanocomposites are characterized by two types of transformation (Fig.4-a). The first of them in the temperature range: 450-600^oC is like in previous case due to CO_2 release. In addition, exothermic type of transition may also suggest combustion of isopropanol residues. The second endothermic transition takes place 1200-1300^oC (in case of 10%Al event takes place about approximately 200^oC earlier). MW samples demonstrated similar pattern of behavior in the temperature range from 1200-1300^oC as the SG samples. The TG curves show that MW powders uniformly lose mass up to 600^oC (Fig.4.-

c). The loss of mass is proportional to the amount of Al_2O_3 phase. This is in contrary to the SG samples. The higher content of Al, the greater mass loss of nanocomposite.

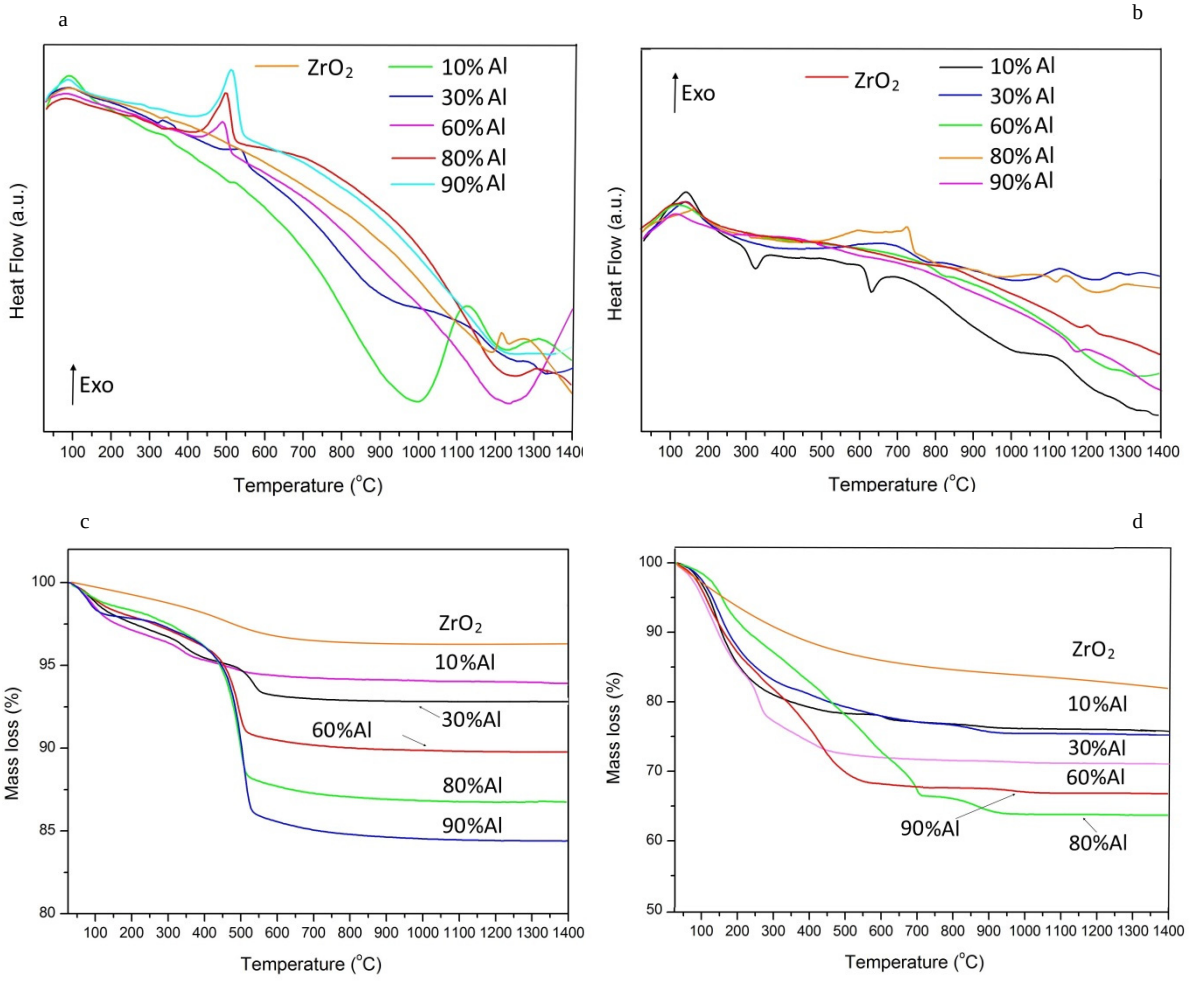

Figure 4. DSC-TG curves for ZrO_2-Al_2O_3 composites. Fig.4 (a) is DSC, and (c) TG for powders synthesied by MW method. Data obtained for powders synthesised by SG method where (b) is DSC, and (d) TG.

3.2. Characteristics of ZrO_2-Al_2O_3 nanocomposites after heating up to 1450°C

All samples produced by MW and SG synthesis and further heat treatment up at 1450 ℃ were found to be crystalline yielding sharp diffractograms (Fig.5.). For MW nanopowders ZrO_2 and 10%Al (9.6 % mol Al in the table 3) powders show only ZrO_2 as monoclinic single phase. Corundum (αalumina) and tetragonal zirconia phases increase when the Al amount rises. (see Fig.5 c-d). According to the author experience [18], a treatment at 1300 ℃ for over 1 h is sufficient for complete segregation of alumina from zirconia. At this temperature alumina is obtained as αalumina [18].

Nanocomposites produced by SG method show that the amount of the tetragonal zirconia increased with rising Al amount. Exception is sample 6 (prepared as 90 mol % Al), where the amount of corundum also increased with

rising Al amount. However, it was visible only for the sample 4 and 6 where segregation of significant amount of corundum took place. Fig. 5-b shows that the sample with ~30 mol % Al is almost pure monoclinic zirconia. The 2 samples with the highest amount of Al included some contamination, probably due to $NaNO_3$ present.

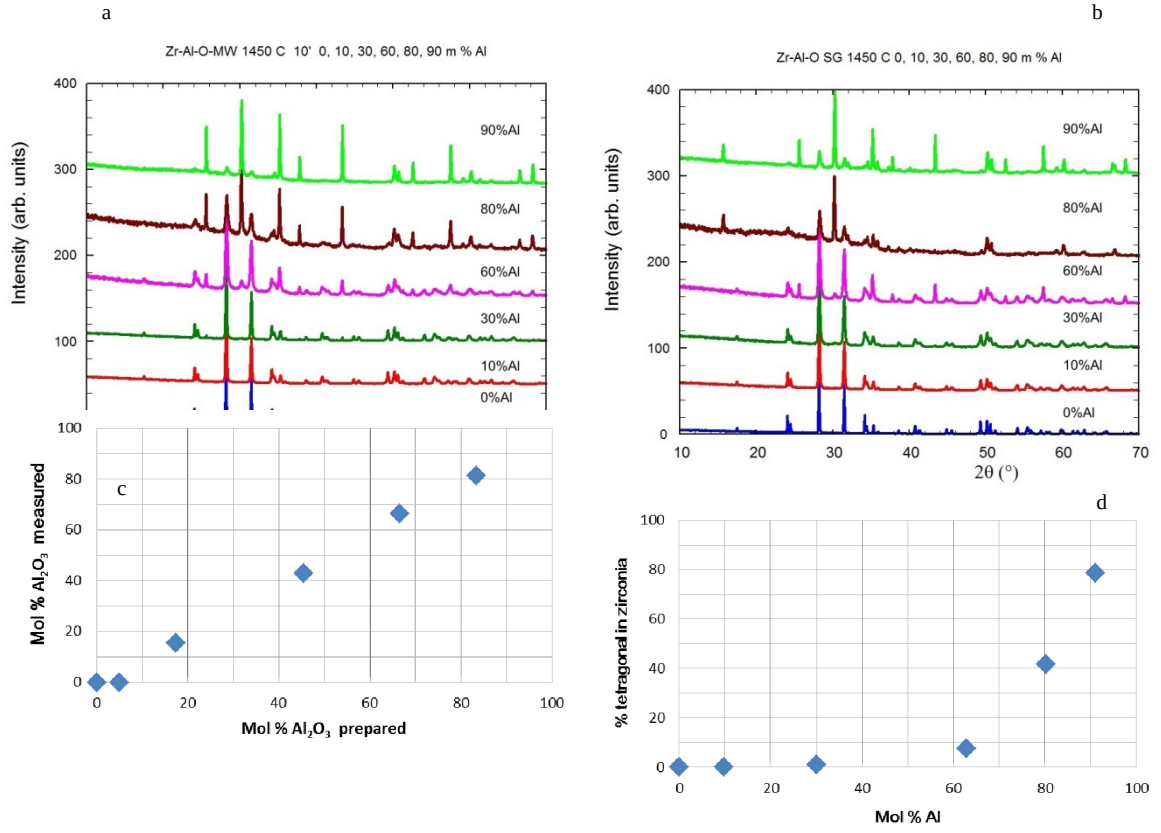

Figure 5. XRD patterns for ZrO_2-Al_2O_3 MW (a), and SG (b) powders after heating up to 1450°C. Pure Zr is in the bottom and 90 mol % Al is in the top. (c) Comparison between measured and prepared Al_2O_3 amount (MW-1450), (d) Percentage of the tetragonal structure in the zirconia phases (MW-1450).

The as-synthesied MW samples showed much faster kinetics for zirconia production than the SG samples. Whereas in MW synthesis the zirconia was formed as nano crystalline powders, the SG synthesis resulted in quasi amorphous zirconia ones. Except for one case where an $Al(OH)_3$-bayerite was formed. By using both synthesis methods Al precipitated as Boehmite. However, in MW powders the Boehmite was with large grains, and the Boehmite grains of the xerogels were nanometric. At all samples with crystalline zirconia it is shown that Al stabilizes the tetragonal phase. This was observed in both synthesis methods.

Table 3. Amount of phases for MW powders with 1450 ℃ treatments for 10 min.

Sample description in this work	m % Al	m % Al_2O_3 prepared	From Rietveld refinement Wt.% corundum	Wt.% t-ZrO_2	Wt.% m-ZrO_2	m % Al_2O_3 measured	Zr/Al measured
ZrO_2	0.0	0.0	0.0	0.0	100.0	0.00	Pure ZrO_2
10%Al	9.6	5.06	0.0	0.0	100.0	0.00	Pure ZrO_2
30% Al	29.9	17.54	13.3	0.7	86.0	15.64	2.70
60% Al	62.5	45.45	38.2	3.7	58.1	42.76	0.67
80% Al	80.0	66.67	61.9	12.1	25.0	66.25	0.25
90% Al	90.9	83.33	78.2	13.3	8.5	81.26	0.12

Raman spectra for annealing at 1450°C ZrO_2-Al_2O_3 nanopowders obtained by MW, and SG methods are shown in Figure 6. For clarity a spectrum obtained from pure ZrO2 is shown on both plots. Changes in spectrum on MW (a) are observed starting from 60%Al and in spectra from SG (b) powders starting from 80%Al. These peeks (150, 250 and 450cm^{-1}) represent increasing amount of tetragonal phase of ZrO_2. This fact is confirmed by Stefanic et al [20] and our Rietveld refinement (Table 3.). It is worth to note that in case of MW powders heating up to 1450°C lead to appearance of t-ZrO_2 already from 60% of Al.

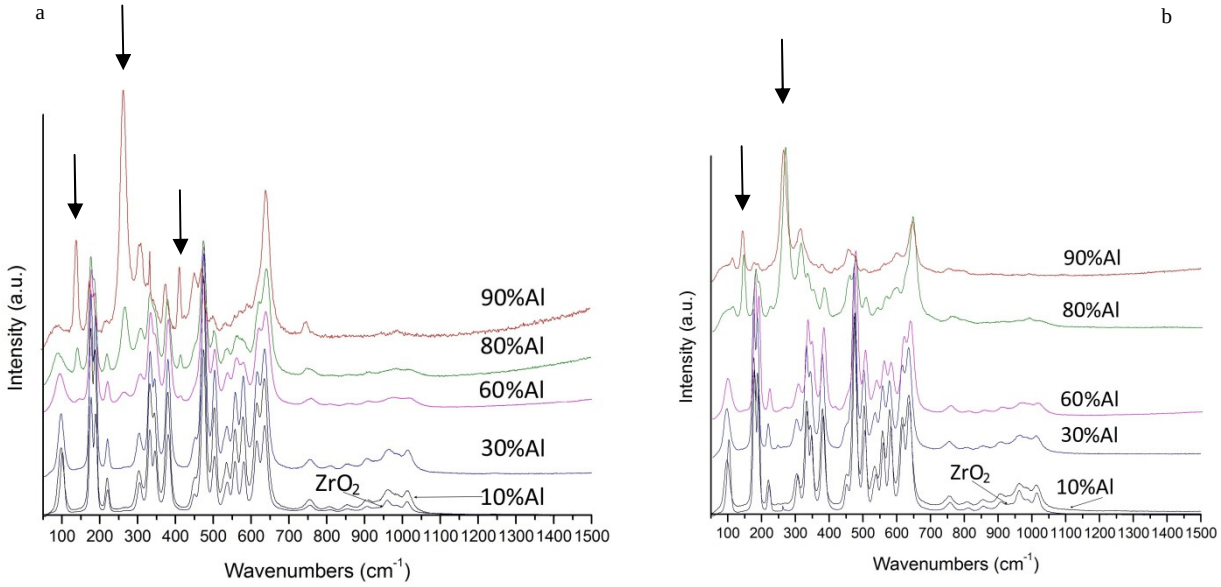

Figure 6. Raman spectra for annealing at 1450°C ZrO_2-Al_2O_3 nanopowders obtained by (a) MW, and (b) SG method.

Figure 7 shows SEM images for SG and MW powders heated up 1450°C. Pictures were made using two detectors: InLens (to the right), and Energy Selective Backscattered -ESB (to the left)- to highlight variety of morphology and chemical composition. The dark phase is Al_2O_3, while the bright one is ZrO_2. In case of MW powders with 10 and 30%Al precipitation of Al_2O_3 phase with the particle size ≤200nm is observed (Figure 7 a-c). SG powders were rich in slightly larger Al_2O_3 particles for these compositions. For SG powders with composition equal to or above 80%Al (Fig. 7-h) morphology of material changes while no morphological change is observed in MW samples. In SG samples over 80%Al Al_2O_3 phase crystalized in elongated, uniform, rod-like particles with the length approximately 600 nm. This is partially due to the difference in mechanism of crystals growth. MW powders goes to the furnace as a crystalline phase, while SG powders crystalize during heating. Unlike SG, the MW nanocomposites form homogeneously distributed phase of ZrO_2 in Al_2O_3 matrix (Fig.7 g-i). Even after annealing at 1450°C ZrO_2 particles stay size below 200nm in size.

4. Conclusions

Our research showed that there is significant difference between nanomaterials obtained using sol-gel method and microwave hydrothermal synthesis. First of all MW method allows to produce uniform nanopowders with narrow particle size distribution. The particle size of MW ZrO_2-Al_2O_3 is found to increase with % Al amount, while in case of SG powders this size is random.

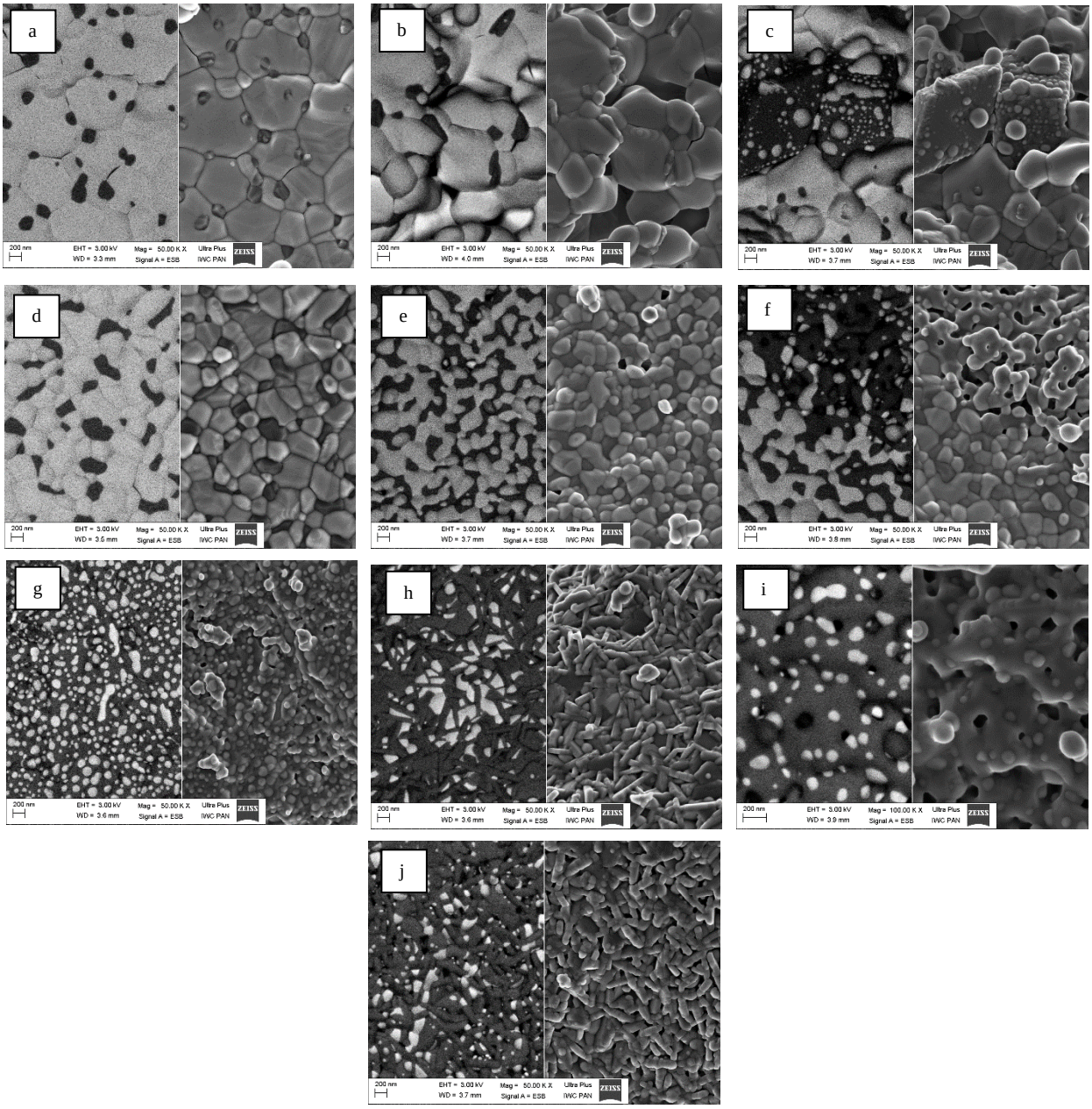

Figure 7 SEM images for nanopowders after heating up to 1450°C in magnification 100 000 obtained by MW method, where (a) is 10% Al, (c) 30%Al, (e) 60%Al, (g) 80%Al, (i) 90%Al. SEM images of nanopowders produced by SG method: (b) 10%Al, (d) 30%Al, (f) 60%Al, (h) 80%Al, and (j) 90%Al.

Morphology of SG and MW nanocomposites remains without changes for compositions up to 30% of Al. For as-synthesised powders the MW samples of 60% Al composition were found to consist of ~20nm spherical nanoparticles while SG samples showed flake-like morphology. Further annealing of powders up to 1450°C does not change significantly morphology in powders with 10-30%Al. In this case particle size based on SEM analysis seems to be approximately 200 nm, while slightly smaller particles are observed for MW powders. Above 80% of Al MW powders have still spherical particles below 200nm, while SG samples are characterized by elongated, rod-like particles. It is known that temperature is a major factor of particles growth in case of ZrO_2-Al_2O_3 nanocomposites. At high temperature the growth rate is high and there is less chance for additional nucleation among the initial

crystals that started to grow and we end with a coarse structure of few large grains [11]. Our findings are in agreement with Deb et al [17] that t- ZrO_2 particles grow inside the pores of the α-Al_2O_3 grains. Samples above 60% Al concentration after annealing show nanocomposite morphology with matrix Al_2O_3 phase hosting small (50-200nm) particles of t-ZrO_2.

In compare to the previous paper [18] this work shows results for ZrO_2 - Al_2O_3 materials obtained with better quality then described in the previous paper. We obtained new nanocomposite material where t- ZrO_2 is stabilized even above 1400°C by Al_2O_3 additive. This material can be synthesized using both MW and SG methods. For lower concentrations of Al solid solution is visible what will be described in details elsewhere.

Acknowledgements

Authors are grateful to the Polish National Science Centre for financial support under contract No. UMO-2013/11/D/ST8/03429- “Sonata 6”.

References

[1] Memorandum of Understanding, For the implementation of a European Concerted Research Action designated as COST Action MP0903 NANOALLOYS AS ADVANCED MATERIALS: from structure to properties and applications. COST 273/09 http://register.consilium.europa.eu/doc/srv?l=EN&f=ST%20273%202009%20INIT.
[2] D. Millers, L. Grigorjeva, A. Opalinska, W. Lojkowski. Solid State Phenom.94 (2003) 135-140.
[3] S. Inamura, H. Miyamoto, Y. Imada, M. Takagawa, K. Hirota, O. Yamaguchi J. Mater. Sci. 29 (1994) 4913–4917.
[4] J.S. Hong, S.D. De la Torre, K. Miyamoto, H. Miyamoto, L. Gao, Mater. Lett. 37 (1998) 6–9.
[5] C.J. Wang, C.Y.Huang, Y.C.Wu, Ceram.Int. 35 (2009) 1467-1472.
[6] W.H. Tuan, J.Eur.Ceram.Soc. 22 (2002) 2827–2833.
[7] J.R. Kelly, I.Denry, Dent. Mater. 24 (2008) 289–298.
[8] A.H. DeAza, J.Chevalier, G.Fantozzi, J. Am. Cer.Soc. (2003), 86 [1] 115–20.
[9] F.A.T. Guimaraes, K. L. Silva, V. Trombini, J.J. Pierri, J. A. Rodrigues, R. Tomasi, E. MJA Pallone, Ceram.Int. 35 (2009) 741-745.
[10] W. Yin, B.Meng, X.Meng, X.Tan, J.Alloys Compd. 476 (2009) 566–570
[11] R. Benzaid, et al Biomaterials 29 (2008) 3636-3641
[12] J. Chandradass, M.H.Kim, D.S.Bae, J.Alloys Compd. 470 (2009) L9
[13] Z. Wei, H. Li, X. Zhang, S. Yan, Z. Lv, Y. Chen, M. Gong,l J.Alloys Compd. 455 (2008)
[14] I. Levin & D. Brandon, J. Am. Ceram. 81 (1998) 1995-2012.
[15] A. Navrotsky, Geochem. Trans., 4 (2003) 34-37.
[16] S. Tsunekawa Ito, S., Kawazoe, Y. & Wang, J.-T., Nano Lett., 3 (2003) 871-987.
[17] A.K. Deb, P. Chatterjee, S.P. Sen Gupta, Mater.Sci. Eng. A 459 (2007) 124–131
[18] G. Kimmel . Zabicky, R. Shneck, A. Tsinman, Z. Shalle, J. D. Fidelus, S. Gierlotka, W. Lojkowski Z. Kristallogr. Proc.1 (2011)455-460.
[19] A. Opalinska, I. Malka, W. Dzwolak , T.Chudoba , A. Presz and W. Lojkowski1 Beilstein J Nanotech. 6 (2014) 27-35.
[20] G. Stefanic, S. Musić, S. Popović, A. Sekulić, J.Mol.Struct. 408-409 (1997) 391–394.
[21] M. Yashima, K Ohtake, M Kakihana, H Arashi, M Yoshimura, J.Phys.Chem.Solids 57 (1996) 17-24.
[22] G. Watson, W. Daniels, C.J. Wang, Appl. Phys.52 (1981) 956-978.
[23] K. Nagabhushana, B. Lakshminarasappa, F. Singh, Bull. Mater. Sci.31 (2009) 669.
[24] A. Boumaza, A. Djelloul,. J. Solid State Chem. 183 (5) (2010) 1063-1070.